Performance Characterization and Simulation of Amine-Based Vacuum Swing Sorption Units for Spacesuit Carbon Dioxide and Humidity Control

Michael J. Swickrath*, Carly Watts† and Molly Anderson‡

NASA Johnson Space Center, Houston, TX, 77058

Summer McMillin§, Craig Broerman¶, Aaron Colunga‖ and Matthew Vogel**

Engineering and Science Contract Group - Jacobs Engineering, Houston, TX, 77058

Controlling carbon dioxide (CO_2) and water (H_2O) vapor concentrations in a space suit is critical to ensuring an astronauts safety, comfort, and capability to perform extra-vehicular activity (EVA) tasks. Historically, this has been accomplished using lithium hydroxide (LiOH) and metal oxide (MetOx) canisters. Lithium hydroxide is a consumable material that requires priming with water before it becomes effective at removing carbon dioxide. MetOx is regenerable through a power-intensive thermal cycle but is significantly heavier on a volume basis than LiOH. As an alternative, amine-based vacuum swing beds are under aggressive development for EVA applications. The vacuum swing units control atmospheric concentrations of both CO_2 and H_2O through fully-regenerative process. The current concept, referred to as the rapid cycle amine (RCA), has resulted in numerous laboratory prototypes. Performance of these prototypes have been assessed experimentally and documented in previous reports. To support developmental efforts, a first principles model has also been established for the vacuum swing sorption technology.

For the first time in several decades, a major re-design of Portable Life Support System (PLSS) for the extra-vehicular mobility unit (EMU) is underway. NASA at Johnson Space Center built and tested an integrated PLSS test bed of all subsystems under a variety of simulated EVA conditions of which the RCA prototype played a significant role. The efforts documented herein summarize RCA test performance and simulation results for single and variable metabolic rate experiments in an integrated context. In addition, a variety of off-nominal tests were performed to assess the capability of the RCA to function under challenging circumstances. Tests included high water production experiments, degraded vacuum regeneration, and deliberate valve/power failure and recovery.

*Analyst, Crew and Thermal Systems Division, 2101 NASA Parkway, EC211, Houston, TX, 77058, AIAA Member.

†Project Engineer, Crew and Thermal Systems Division, 2101 NASA Parkway, EC211, Houston, TX, 77058, AIAA Member.

‡Analysis Lead, Crew and Thermal Systems Division, 2101 NASA Parkway, EC211, Houston, TX, 77058, AIAA Member.

§Project Engineer, EVA and Health Systems Group, 2224 Bay Area Blvd., Houston, TX, Member AIAA.

¶Project Engineer, Advanced Systems Group, 2224 Bay Area Blvd., Houston, TX, Member AIAA.

‖Project Engineer, Advanced Systems Group, 2224 Bay Area Blvd., Houston, TX, Member AIAA.

**Thermal Analyst, Thermal and Environmental Analysis Group, 2224 Bay Area Blvd., Houston, TX, Member AIAA.

Nomenclature

acfm	= Absolute cubic feet per minute
BET	= Brunauer-Emmett-Teller
CO_2	= Carbon dioxide
EMU	= Extravehicular mobility unit
EVA	= Extravehicular activity
GN2	= Gaseous nitrogen
H_2O	= Water
LiOH	= Lithium hydroxide sorbent
MetOx	= Metal oxide sorbent
PGS	= Pressure garment suit
PLSS	= Portable life support system
psia	= Pounds per square inch absolute
psid	= Pounds per square inch differential
RCA	= Rapid cycle amine
RPM	= Revolutions per minute
SA9T	= Proprietary sorbent developed by Hamilton Sundstrand
SLM	= Standard liters per minute
SWME	= Spacesuit water membrane evaporator

I. Introduction

During extra-vehicular activity (EVA), the metabolic work load of an astronaut is typically increased resulting a commensurate increase in CO_2 and H_2O production. These compounds rapidly concentrate within the closed volume of the spacesuit if not properly managed through the ventilation subsystem of the Portable Life Support System (PLSS). Traditionally, the extra-vehicular mobility unit (EMU) PLSS designed in the 1970s and 1980s accomplishes this task by using consumable lithium hydroxide (LiOH) canisters (2.9 kg or 6.4 lb_m) and a condensing heat exchanger (3.3 kg or 7.3 lb_m).[1–3] Alternatively, regenerable metal oxide (MetOx) canisters (15.5 kg or 34.2 lb_m) have been developed to overcome the logistical challenges associated with shipping a multitude of LiOH canisters to support International Space Station (ISS) based EVAs. However, regeneration requires a power intensive 14 hour baking procedure rendering the mass-power trade less attractive.

Alternatively, an on-the-back vacuum-regenerable concept based on an amine sorbent referred to as the rapid cycle amine (RCA) is under development by Hamilton Sundstrand (Windsor Locks, CT). The RCA accomplishes simultaneous carbon dioxide and humidity control, thereby eliminating the need for the condensing heat exchanger. The amine sorbent, referred to as SA9T by Hamilton Sundstrand, is a proprietary formulation developed from a material with primary and secondary amine groups that selectively remove CO_2 and H_2O in the ventilation stream. The reaction mechanism for amine-based sorption has been proposed in detail elsewhere.[4–6] In particular, three reactions appear to occur in parallel.[5]

$$CO_2 + 2R_2NH_2^+ \rightarrow R_2NH_2^+ + R_2NCOO^- \tag{1}$$

$$CO_2 + 2H_2O + R_2NCOO^- \rightarrow R_2NH_2^+ + 2HCO_3^- \tag{2}$$

$$CO_2 + H_2O + R_2NH \rightarrow R_2NH_2^+ + HCO_3^- \tag{3}$$

The first reaction demonstrates the formation of a carbamate group which can be further reacted with water to form bicarbonate in reaction (2). Reaction (1) is seemingly the primary reaction involved in solid-phase loading as suggested by Goeppert et al.,[4] with the demonstration of only a slight increase in loading capacity in humid environments. Moreover, a deliberate conversion of primary amine groups to secondary amines purportedly aids in ambient temperature vacuum regeneration.[5]

A recent prototype of the RCA has been developed for 3.84 kg total test article mass. This is a considerable mass savings when compared to the LiOH or MetOx systems requiring the supplementary condensing heat exchanger. The technology development prototype has been thoroughly tested in a PLSS ventilation system test bench for a wide range of metabolic rates, gas flow rates, and system pressures relevant to EVA.[7–9] The test article has proven capable of revitalizing the atmosphere under expected EVA conditions. However, the test article has not been tested in conjunction with the flight-like ventilation fan, and the components of the oxygen and thermal subsystems, all of which could conceivably impact test article performance through temporarily altering system temperature or pressure. As a result, integrated testing is necessary to fully understand the performance of the RCA within the advanced PLSS. Moreover, a number of off-nominal conditions could plausibly occur during an EVA which the RCA will need to overcome to ensure the safety of the astronaut.

The PLSS 1.0 integrated test bed was designed, built, and operated in 2011 to better understand the performance capabilities of the advanced PLSS under development at Johnson Space Center. The results described herein focus predominantly on the performance of the RCA swing bed within the PLSS 1.0 ventilation subsystem. In addition to exploring performance under anticipated nominal conditions, a transient EVA metabolic profile was simulated, high water production rates were explored, loss of vacuum performance was analyzed, and the capability to recover from the loss of power to the RCA valve was also investigated.

II. Experimental

The advanced PLSS incorporates a number of subsystem components designed deliberately to increase component and subsystem reliability and robustness, decrease consumables use, and develop an adaptable exploration platform while NASA continues to consider a multitude of destinations under a flexible path program. NASA developed the PLSS 1.0 test stand to simulate the capabilities of the advanced PLSS schematic[1,3] representing the first time the advanced PLSS concept was assembled and tested in an integrated configuration. The schematic of the test stand is illustrated in Fig. 1 and demonstrates the (1) high-pressure oxygen delivery system, (2) the ventilation system, and (3) the thermal control system. The subsequent sections of this report will discuss each subsystem in limited detail.

A. High-Pressure Oxygen Delivery System

The oxygen system is responsible for delivering gas for respiration to the crew member as it is metabolically consumed across a wide variety of suit pressures. This is accomplished using primary and secondary variable pressure regulators fabricated by Carleton Technologies, Inc. (Orchard Park, New York). The two-stage electromechanical regulators can accomplish regulation from 3750-250 pounds per square inch absolute (psia) in the first stage. The second stage regulates between 0-8 pounds per square inch differential (psid) referencing pressures between 0-14.7 psia. The regulators have between 3600-4000 set points within the described range to provide high precision pressure control compared to the current EMU PLSS control module which can only operate at two distinct set points.

B. Thermal Control System

The thermal control system maintains a comfortable environment for the astronaut while also cooling the avionics associated with the PLSS. This is accomplished primarily through evaporative cooling via provided by the spacesuit water membrane evaporator (SWME). The SWME is operable across a broad range of inlet and outlet pressures, can tolerate gas bubbles acting as an *in situ* degasifier, and is relatively insensitive to water quality meeting performance requirements with potable water containing particulate matter.[10–12]

C. Ventilation System

The ventilation system has several important components that are relevant to the performance of the RCA. The ventilation system fan developed by Hamilton Sundstrand (Windsor Locks, CT) was designed to provide 4.5-6.0 absolute cubic feet per minute (acfm) flow at 35,000-45,000 revolutions per minute (RPM) at 4.3 psia. The fan can achieve speeds as high as 70,000 RPM to provide up to 8.0 acfm flow under contingency conditions.

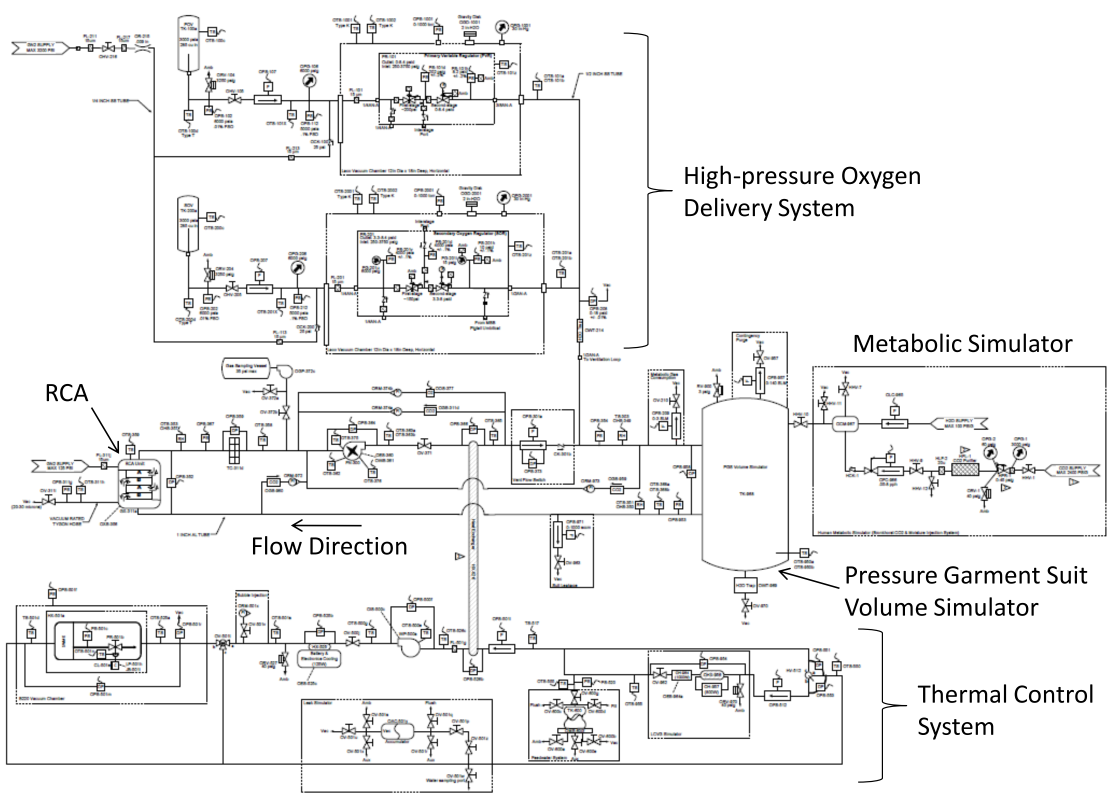

Figure 1: Schematic for the PLSS 1.0 integrated test bed.

A large open tank is also part of the ventilation system simulating the open-volume of the spacesuit at roughly 2.0 cubic feet. A Bronkhorst (Bethlehem, PA) controlled evaporator and mixing system is connected to the spacesuit pressure garment suit (PGS) volume simulator to introduce metabolically relevant amounts of CO_2 and H_2O vapor. A port located just upstream of the volume simulator introduces 'breathing' gas to the system, using nitrogen as a surrogate for oxygen for safety purposes. Another port, situated in between the gas introduction port and PGS volume simulator, simulates metabolic consumption as gas is drawn from the system. A third port, located downstream the volume simulator, represents suit leakage as gas is drawn from the system. Carbon dioxide sensors, humidity sensors are located at the RCA inlet, RCA outlet, and PGS volume simulator inlet. In addition, flow meters are located within the ventilation system for complete characterization of flow within the loop enabling the team to assess the performance characteristics of the RCA.

PLSS 1.0 Ventilation Analytical Model

A model of the PLSS 1.0 ventilation system has been developed in tandem to testing in the Aspen Custom Modeler software package (Aspen Technology, Inc.; Burlington, MA). The model is described in detail in previous manuscripts.[9] The flow diagram of the model is represented in Fig. 2. The gaseous nitrogen (GN2) blocks introduce make-up gas to the system as it is metabolically consumed or removed from the system through ullage losses associated with the vacuum swing process. The PGS volume simulator is modeled as a continuously-stirred tank reactor that implicitly assumes good mixing is achieved. The inlet and outlet concentrations to the PGS during the experiment indicate that this is a reasonable assumption. The mixer and evaporator metabolic simulator is modeled as separate sources converging in an adiabatic mixer. The rapid cycle amine model is comprised of individual layers of the two-bed system along with valving to segregate flow depending on which bed is undergoing vacuum regeneration versus scrubbing the process flow stream. The bed layer model employs an axially-dispersed plug flow material balance with an accompanying energy balance to simulate mass exchange between vapor and solid phases.[9] The Aspen Custom Modeler software decomposes the system of coupled partial differential equations into a system of algebraic and ordinary differential equations through advanced linear algebra. Solutions were achieved through fourth-order central finite differencing schemes with teh GEAR formulae for numerical integration. The GEAR formulae were chosen according to its ability to handle numerically stiff problems where relevant time-scales can vary on several orders of magnitude. This is necessary since transitions from adsorption to vacuum regeneration result in compressible flow for fractions of a second while the adsorption process takes several minutes in comparison.

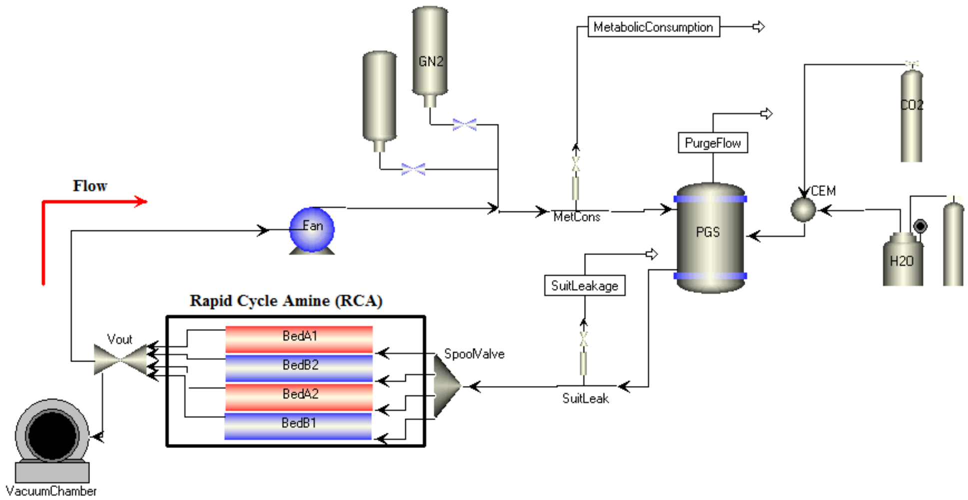

Figure 2: Analogous flow diagram for the PLSS 1.0 ventilation sub-system model.

III. Results and Discussion

The PLSS 1.0 integrated test stand was built to assess performance of subsystem components operating in series and parallel under nominal, off-nominal, and contingency operations. The priority was to fully instrument the apparatus for complete performance characterization rather than attempt to package the system. A photograph of the resulting test stand is shown in Fig. 3 and demonstrates the electronics and data acquisition system (left), the ventilation system (middle top level), thermal control system (middle lower level), and the SWME and vacuum chamber (right).

A. Single Metabolic Rate Experiment

Steady state metabolic output was simulated using constant CO_2 and H_2O injection in an effort to satisfy primary objectives of demonstrating performance requirements across different pressures and metabolic rates. Furthermore, these tests serve to functionally verify that the test apparatus and associated instrumentation were reporting reasonable results. Data were compared to several single metabolic rate tests that were investigated in previous studies.[7–9] In these tests, the loop flow rate was between 4.5-6.0 acfm, loop pressure was either 4.1, 6.0, or 8.0 psia, and the metabolic rate was varied between 400, 1000, and 1600 British thermal units (Btu/hr). CO_2 was allowed to rise within the test loop until it reached 6.0 millimeters of Mercury (mm Hg) at the PGS volume simulator inlet before commanding the RCA valve to actuate and switch from the saturated bed to the vacuum-regenerated bed. The value of 6.0 mm Hg was derived from the Constellation Program 8 hour CO_2 exposure requirement.[13] 7.6 mm Hg with margin added to provide some guard-band against crossing that lower threshold. Moreover, this threshold was chosen because it had been previously tested and, therefore, data exist to compare these results. This provides the means to diagnose any immediate anomalies that are observed from the new test data. Simulated metabolic rate test points proceeded until a repeating pattern occurred in the transient partial pressure profiles of CO_2 and H_2O which we refer to as 'cyclic steady-state'. This was quantitatively evident when the time-to-cycle the valve became constant. The time-to-cycle is referred to as 'half-cycle' time since two valve cycling events takes you from a particular bed in scrubbing mode to regeneration mode and then back to scrubbing mode. As an additional measure, a global moving average was calculated with the cyclic data to verify the slope of

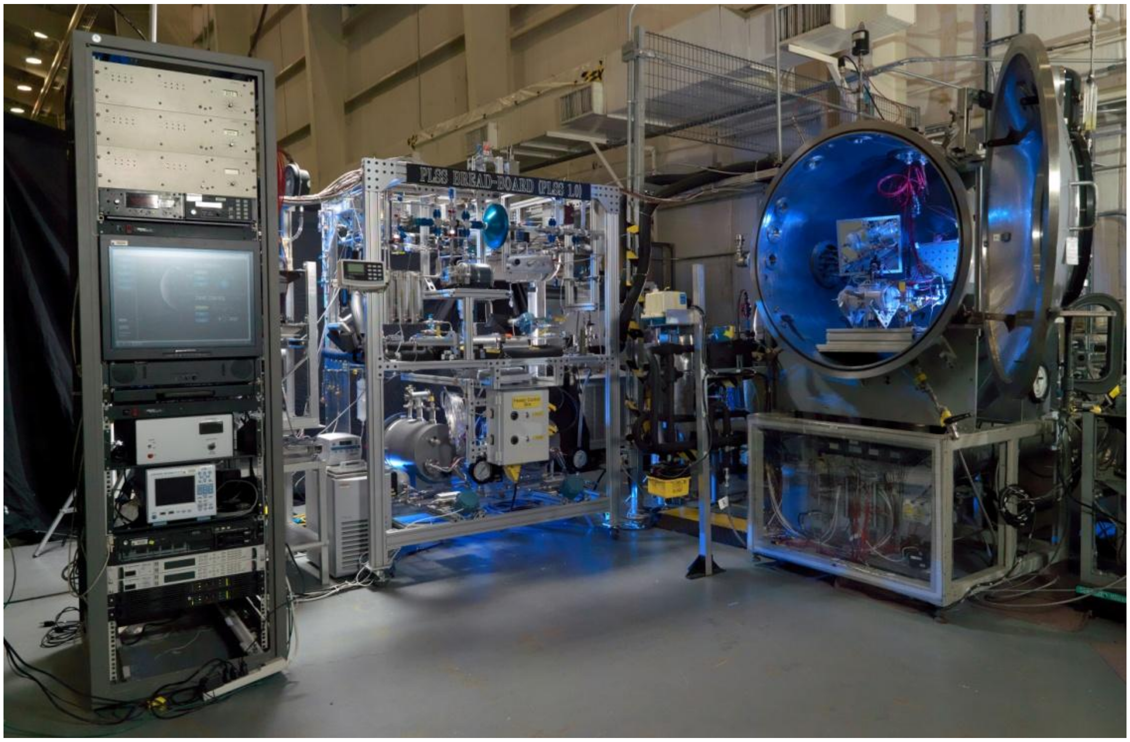

Figure 3: PLSS 1.0 integrated test stand.

the average asymptotically approaches zero as cyclic steady-state was approached. Typical results for this type of an experiment are displayed in Fig. 4.

The results in Fig. 4 demonstrate the RCA swing bed was indeed capable of revitalizing the atmosphere of the spacesuit at a simulated metabolic rate of 1000 Btu/hr. The average CO_2 partial pressure returning to the helmet from the RCA was 3.35 mm Hg when cycled at an instantaneous threshold of 6.0 mm Hg leading to an average half-cycle time of 3.55 min. The RCA outlet dew point averaged 12.7 °F which is below the 32.5 °F indefinite relative humidity tolerance defined by the Constellation Program[13] and is closer to the 2 hour exposure limit (3.7-20.2 °F). Consequently, these conditions are somewhat dryer than desirable. It is worth mentioning that the RCA was configured in a single-end inlet regeneration mode which corresponds to pulling a vacuum at the inlet port during regeneration. Previous testing indicated that this leads to dryer swing bed outlet streams than single-end outlet regeneration.[8,9] While the primary requirement of minimizing CO_2 partial pressure was met, the secondary requirement of maintaining comfortable humidity levels was not quite attained. Work is underway to develop a better understanding of how to meet the secondary goal through re-orienting the RCA or through enhanced control algorithms that provide a better balance between low CO_2 and increased humidity.

B. Variable Transient Metabolic Rate Experiment

The single metabolic rate experiments lend insight into how the RCA will perform under static conditions. However, EVA is rarely static and can vary over a wide range of metabolic rates. Consequently, it is important to characterize the capability of the RCA to transition rapidly to new metabolic challenges. The goal of the next phase of the investigation was to explore the RCA performance through simulated EVA variable metabolic rate experiments. The selected metabolic profile is indicated in table 1. It should be noted that the average metabolic rate for this profile is 1330 Btu/hr which is approximately 30% higher than what is typically expected for a typical EVA (*i.e.* approximately 1000 Btu/hr). As a result, this test presents a considerable challenge to the RCA and advanced PLSS concept as a whole.

There has been recent discussion regarding lowering CO_2 partial pressure threshold and the impacts the new threshold may impose upon life support systems as a result.[14] To assess the performance of the PLSS

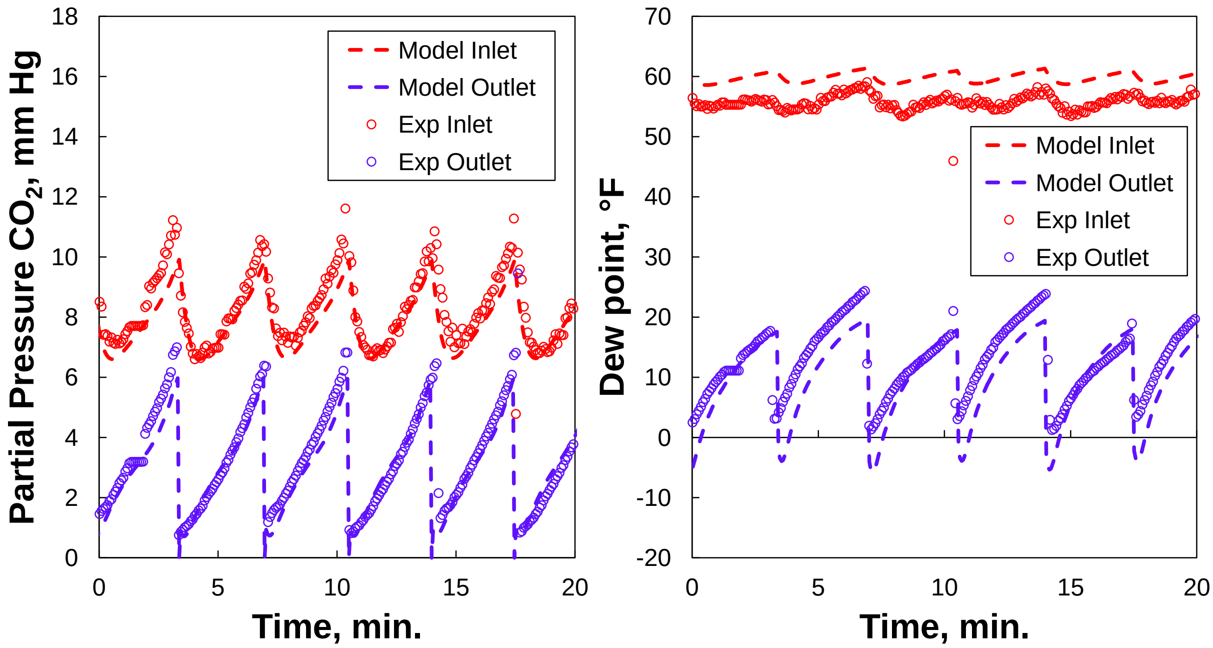

Figure 4: Typical results for a single metabolic rate experiment. Test conditions include a metabolic rate of 1000 Btu/hr, 4.1 psia loop pressure, and a 4.5 acfm flow rate. The RCA valve was cycled when the PGS volume simulator inlet CO_2 partial pressure reached 6.0 mm Hg.

simulator under such constraints, the RCA was cycled when the PGS volume simulator inlet CO_2 partial pressure reached and instantaneous value of 3.0 mm Hg, one half of the previous value of 6.0 mm Hg. Results of this test, along with analytical model simulation results, are presented in fig 5.

As indicated in Fig. 5, the RCA was capable of revitalizing the atmosphere during the variable metabolic rate experiment. The RCA accommodated lower carbon dioxide threshold albeit the valve had to cycle fairly quickly at times (as short as 29.5 seconds for the 2390 Btu/hr period). Although not demonstrated in Fig. 5, metabolic rates as high as 3070 Btu/hr were tested in which the RCA continued to demonstrate the capability to maintain safe CO_2 concentrations although cycle time did decrease to 20.5 seconds. The mean partial pressure returned from the RCA to the PGS volume simulator during this test was 2.14 mm Hg. The inspired partial pressure of CO_2 would presumably increase slightly and is a function of mixing achieved within the helmet design (see Ball & Straus, 2011[15]) that is still undergoing optimization. This resulted in a fairly dry PGS volume simulator inlet stream with a dew point of 2.6 °F on average with fluctuations between -15 °F to 15 °F. The mean dew point within the PGS simulator was considerably higher at 53.2 °F. The inlet and outlet CO_2 concentration and dew point from the model seem to agree relatively well with the experiment.

The model predicted slightly shorter half-cycle times for low metabolic rates and longer times for higher metabolic rates. These differences are notable because previous modeling of independent RCA testing was capable of predicting half-cycle time very well.[9] It is suspected that the discrepancy in half-cycle time predictions is attributed to the phenomenological vacuum system model that relies on choked-flow and non-choked continuum flow equations. These equations require a minimum achievable pressure for the vacuum system which was set as a constant in this analysis.[9] In reality, the minimum attainable pressure achievable by the vacuum system is a function of the mass flow entering the vacuum system. For the RCA, the mass flow was typically on the order of a gram/minute across all metabolic rates, which does not significantly alter the minimum attainable vacuum pressure enough to discernibly influence performance when it is tested by itself. However, the SWME releases on the order of 2 g/min to 40 g/min. of water into the vacuum system which did significantly influence vacuum system performance as both the RCA and SWME were routed to the same vacuum chamber for PLSS 1.0. Future work is underway to increase the fidelity of the vacuum regeneration portion of the model to improve half-cycle time prediction at the metabolic rate extremes.

Table 1: Seven-hour Variable Metabolic Profile Experiment for the PLSS 1.0 integrated test.

Sequence [No.]	Met. Rate [Btu/hr]	Flow Rate [acfm]	CO_2 Injection [SLM]	H_2O Injection [g/hr]	Duration [min]
1	1600	6.0	1.43	83.7	60
2	680	6.0	0.54	66.4	30
3	2390	6.0	1.95	75.0	30
4	1020	6.0	0.81	83.5	30
5	1540	6.0	1.22	89.7	30
6	1130	6.0	0.89	86.9	30
7	1880	6.0	1.49	80.8	30
8	680	6.0	0.54	66.4	30
9	850	6.0	0.68	76.2	30
10	1370	6.0	1.08	90.2	30
11	680	6.0	0.54	66.4	30
12	1600	6.0	1.43	83.7	60

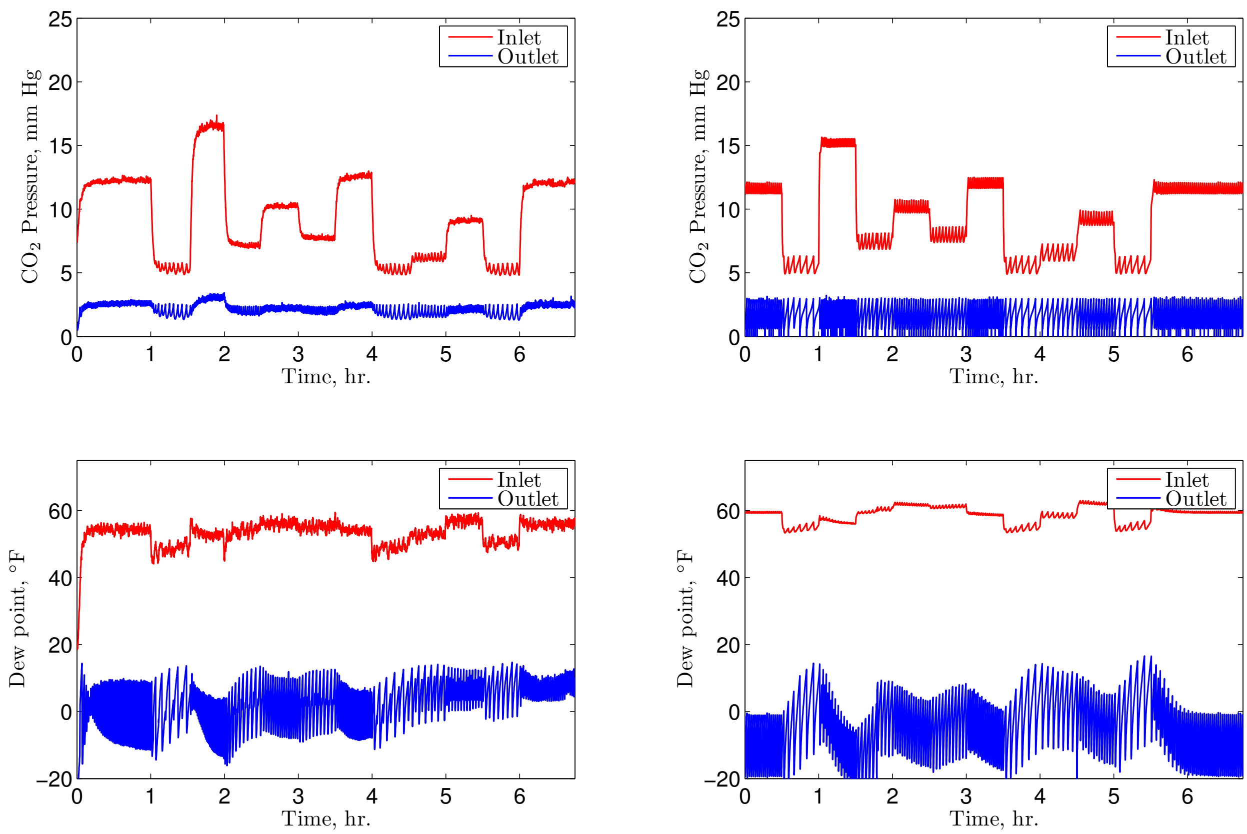

Figure 5: 7-hour variable metabolic rate experiment (left) and simulation results for comparison (right). Test conditions include a mean metabolic rate of 1330 Btu/hr, 4.1 psia loop pressure, and a 4.5 acfm flow rate. The RCA valve was cycled when the PGS volume simulator inlet CO_2 partial pressure reached 3.0 mm Hg.

C. Increased Water Vapor Production Experiment

The previous investigations demonstrated the RCA vacuum swing sorption system is capable of revitalizing the atmosphere within the spacesuit across a broad range of metabolic rates in the integrated test. These results are encouraging from a developmental perspective. However, it is not uncommon that unexpected circumstances that are not accounted for in the design phase arise during EVA. After the primary objectives of the integrated test were met, a great deal of time was spent exploring some other unexpected, although plausibly possible, scenarios. The detailfirst of these explored RCA performance versus increased water vapor loading.

In this test series, the expected water production rates were increased incrementally to nearly twice the nominal crew production rate. The liquid cooling ventilation garment in the spacesuit is responsible for keeping the astronaut cool and can also function as a condensing heat exchanger when the flow rate is high and the coolant temperatures are low. This limits the amount of water vapor experimentally observed in the spacesuit gas volume with the current EMU.[16] High humidity test series injected CO_2 at rates equivalent to 400–1600 Btu/hr metabolic rates with the flow rate of 4.5 acfm at 4.1 psia system pressure. Typical results for the 1000 and 1600 Btu/hr experiments are illustrated in Fig. 6.

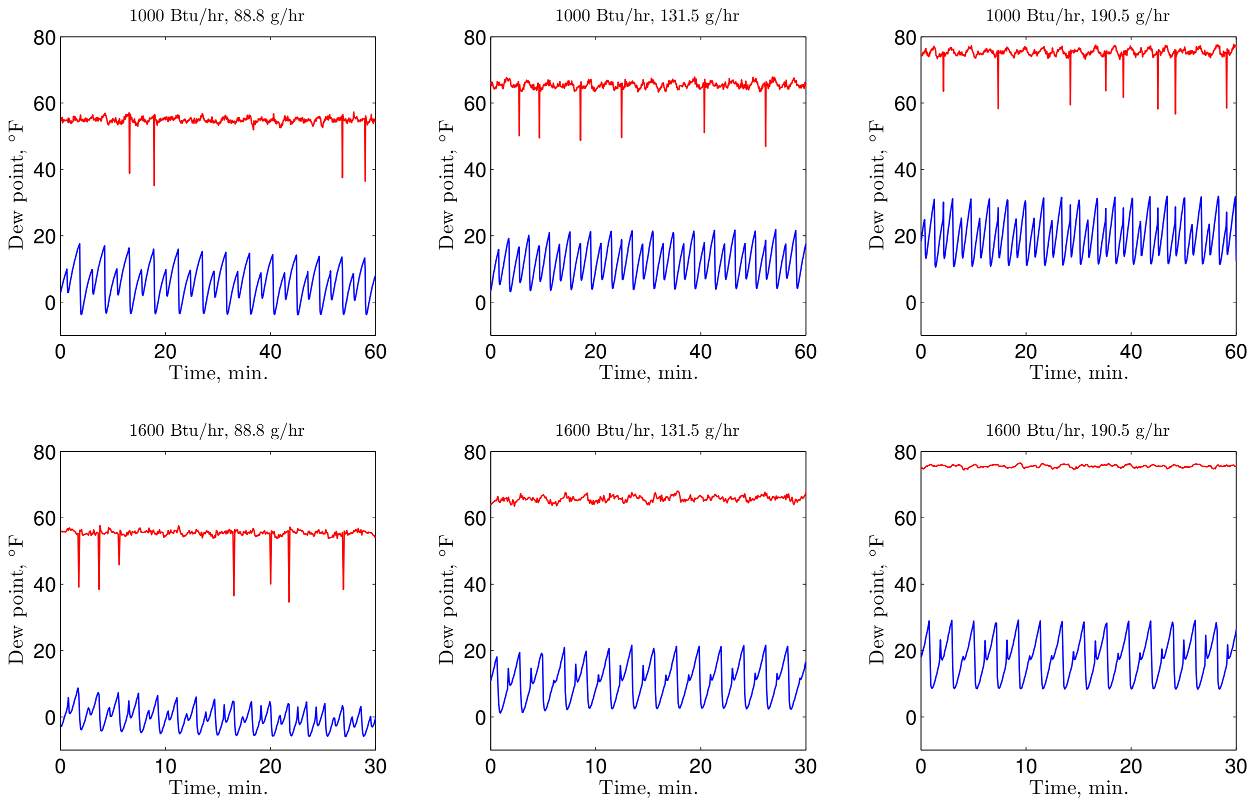

Figure 6: High humidity experimental results for several water production rates and metabolic rates.

As demonstrated in Fig. 6, the RCA was capable of air revitalization as water vapor production rate increased. For the near-nominal cases (left column, 88.8 g/hr), the PGS simulator dew point was around 55 °F with a PGS volume simulator inlet stream between 0-20 °F favoring increased humidity for the lower metabolic rate. As the water vapor production rate increased for a constant metabolic rate (middle column, 131.5 g/hr; right column, 190.5 g/hr), the outlet stream of the RCA contained increasingly more moisture with a commensurate increase in the moisture in the PGS simulator. At the highest water vapor production rates (right column, 190.5 g/hr), the PGS volume simulator has dew points near gas temperature indicating near 100% humidity. In the highest humidity cases, it is plausible that condensation could be occurring within the test loop. This was seemingly confirmed by mass balance calculations with the test data which indicate the injection rate is higher than the removal rate by a several percent for the 190.5 g/hr cases.

Another trend illustrated by the data is that the dew point into and out of the RCA is different from bed-to-bed. The cause of this behavior is not entirely clear. Although sorbent mass may be similar bed-to-bed, channeling may be occurring through one of the beds rendering some of the sorbent inaccessible. Alternatively, if one of the beds starts in a state where it is not completely regenerated relative to the other, the model predicts this type of asymmetry will occur initially before settling out as the experiment time increases over several hours. This could also be the case experimentally, although the data does not show any discernible indication the asymmetry was attenuating. In spite of the asymmetry, this data set is promising with respect to the capability of the RCA to handle water production rates significantly higher than historically observed in the current EMU.

D. Regeneration with Degraded Vacuum

In addition to testing high CO_2 and H_2O production rates, performance was assessed when the vacuum regeneration capability has been intentionally compromised. The integrated test stand employed two HullVac Model HV320 rotary piston vacuum pumps (HullVac; Ivyland, PA) in series with a liquid nitrogen cold trap upstream responsible for removing the majority of the water vapor entering the vacuum system. The vacuum system was capable of achieving pressures at a fraction of a mm Hg even with the increased mass load from the RCA, and with SWME at high simulated metabolic rates. A vacuum line connected the RCA exhaust port to the vacuum chamber (see: Fig. 1), which is serviced by the dual pump/cold trap vacuum system. A valve and line were connected very close to the RCA vacuum line such that ambient laboratory air could be metered to raise the RCA backpressure in a controlled manner. Targeted mean RCA backpressures ranged from 0.5 to 2.8 mm Hg with the actual mean backpressures reaching reached just over 3 mm Hg. Characteristics results from this experiment are displayed in sub-half-cycle detail in Fig. 8.

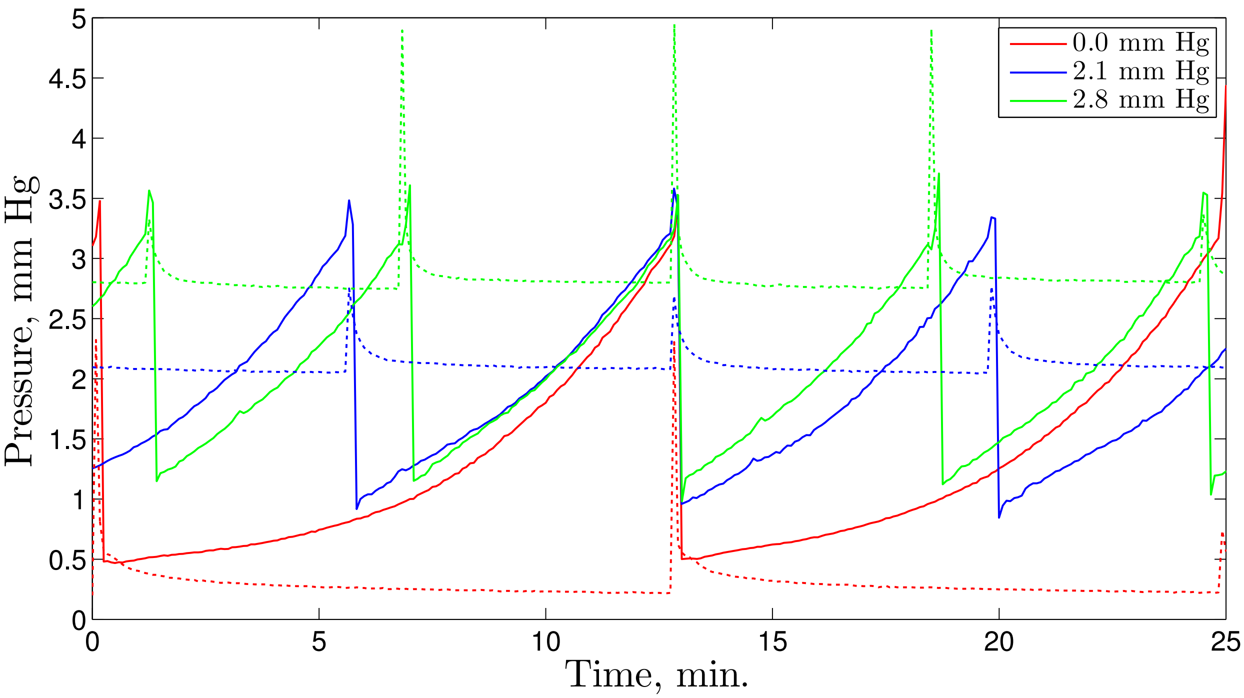

Figure 7: Comparison of results for the degraded vacuum experiments. Test conditions include a metabolic rate of 400 Btu/hr, 4.1 psia loop pressure, and a 4.5 acfm flow rate with nominal vacuum (labeled 0.0 mm Hg), and compromised vacuum with chamber pressures at 2.1 and 2.8 mm Hg. Dashed lines represent the pressure of the RCA vacuum line pressures; solid lines indicate the partial pressure CO_2 at the PGS volume simulator inlet in the ventilation stream. The RCA valve was cycled when the outlet CO_2 partial pressure reached 3.3 mm Hg.

Fig. 8 shows that the half-cycle time is significantly longer for the nominal vacuum case, which is demonstrative of good vacuum quality. As the chamber pressure is increased, the pressure that the RCA reaches during the regeneration cycle is significantly increased, as demonstrated by the dashed lines. Since the loading rate can be approximated as a difference in actual and equilibrium partial pressures from the isotherm data, the increased pressure within the canister directly impacts the rate of desorption. This is manifest in shorter half-cycle times as well as a higher partial pressure of CO_2 at the initiation of the subsequent cycle. In spite of the increase in pressure and decrease in half-cycle time, the RCA is still capable of keeping CO_2 partial pressure below 3.3 mm Hg. These results are encouraging as they suggest the RCA is robust and can still function with a poor vacuum source. Moreover, if vacuum is less than desirable due to blockage, the decrease in half-cycle time provides immediate data to identify the problem and respond during an EVA assuming there is no change in the crew metabolic rates.

A deeper trend is also demonstrated in Fig. 8. At the onset of a regeneration cycle, the two beds of the RCA first equalize to a pressure of 2.05 (*i.e.* 4.1 psia divided by two) and then the adsorb bed enters desorb. During that transition, the ullage gas within the regenerating bed seeing vacuum is quickly removed. This process occurs within a fraction of a second. After the ullage gas leaves the canister comprised mostly of oxygen (or nitrogen in the testing), the adsorbed water and carbon dioxide begin deloading from the solid phase removing any remaining oxygen in the gas-phase as the material flows toward the vacuum source. This process takes from seconds to minutes. At the end of the desorption cycle, the gas phase remaining within the canister will be entirely composed of CO_2 and H_2O in partial pressures that are at equilibrium with the remaining material on the solid phase. This relationship is characterized by respective CO_2 and H_2O adsorption isotherms. The result is that the relative partial pressure CO_2 to vacuum pressure at the end of a cycle and beginning of the next cycle give an indication of the composition of gas within the canister at the end of regeneration phase. For the nominal case, the vacuum pressure versus canister partial pressure of CO_2 at the beginning of the next cycle are nearly overlapping with a slightly higher canister partial pressure (indicating pressure drop between vacuum pressure measurement and actual canister pressure). This suggests the gas within the canister prior to starting the next adsorption cycle is predominantly CO_2 for the nominal case. For the 2.1 mm Hg case, the partial pressure of CO_2 at the start of the next cycle is 0.98 mm Hg which indicates approximately 47% of the remaining material is CO_2. Lastly, for the 2.8 mm Hg case, the partial pressure of CO_2 at the start of the next cycle is 1.15 mm Hg which indicates approximately 41% of the remaining material is CO_2.

To summarize, as pressure is increased, the relative CO_2 to H_2O concentration decreases. This is consistent with the isotherms of CO_2 and H_2O on SA9T described in a previous study.[9] The water isotherm follows Type III behavior describable with Freundlich or Brunauer-Emmett-Teller (BET) relationships.[17,18] The carbon dioxide isotherm is more Type I in nature and is described well by a Langmuir or Toth isotherm.[17,18] A Type III isotherm has the greatest slope for loading versus partial pressure at higher pressures. Alternatively, the Type I isotherm has the greatest slope at low partial pressures. This means that when pressures are low, a small change in partial pressure of H_2O corresponds with a small change in equilibrium concentration of water vapor thereby having only a marginal influence on the driving force for H_2O desorption. Conversely, at low pressures, a small change in partial pressure of CO_2 significantly alters the equilibrium concentration of CO_2 leading to a considerable increase in the driving force for desorption. As a result, the relative composition within the canister changes significantly during the regeneration process. This also indicates vacuum quality is of greatest importance for CO_2 removal which is the primary objective of the RCA. This also supports the consistent trend observed that the RCA tends to over-dry the ventilation air ostensibly because H_2O readily adsorbs to the SA9T and is subsequently desorbed more easily than CO_2. Lastly, it is worth noting that Type I isotherm behavior typically indicates chemisorption where covalent bonds are formed (see eqs. 1– 3) versus non-covalent interactions for Type III physisorption. This is seemingly confirmed with the much increased heat of adsorption for CO_2 versus H_2O (94.0 kJ/mole-K versus 44.0 kJ/mole-K[9]). Consequently, it would be expected that Type I regeneration would necessitate a greater driving force.

Fig. 8 summarizes the rest of the degraded vacuum results across various degraded vacuum pressures. The average vacuum pressure without intentionally compromising the base vacuum pressure was metabolic rate dependent due to the amount of water introduced to the vacuum system by the thermal loop through the SWME. At 400 Btu/hr, the pressure was around 0.29 mm Hg on average increasing to 0.52 mm Hg for the 1600 Btu/hr case. Two trends are observed as the base vacuum is increased from the nominal pressure up to just over 3.0 mm Hg. First, the half-cycle time decreases. This is most apparent for the 400 Btu/hr case. This trend is expected since the cycle time follows an exponential decay function with metabolic rate.[8,9] Second, the mean partial pressure of CO_2 within the ventilation system increases with shorter cycle times which is consistent with the data previously reported.[8] Essentially, vacuum degradation manifests as an artificial increase in metabolic rate when monitoring only the PGS volume simulator inlet partial pressure and half-cycle time. During an actual EVA, care must be taken to not mistake such observations. As a

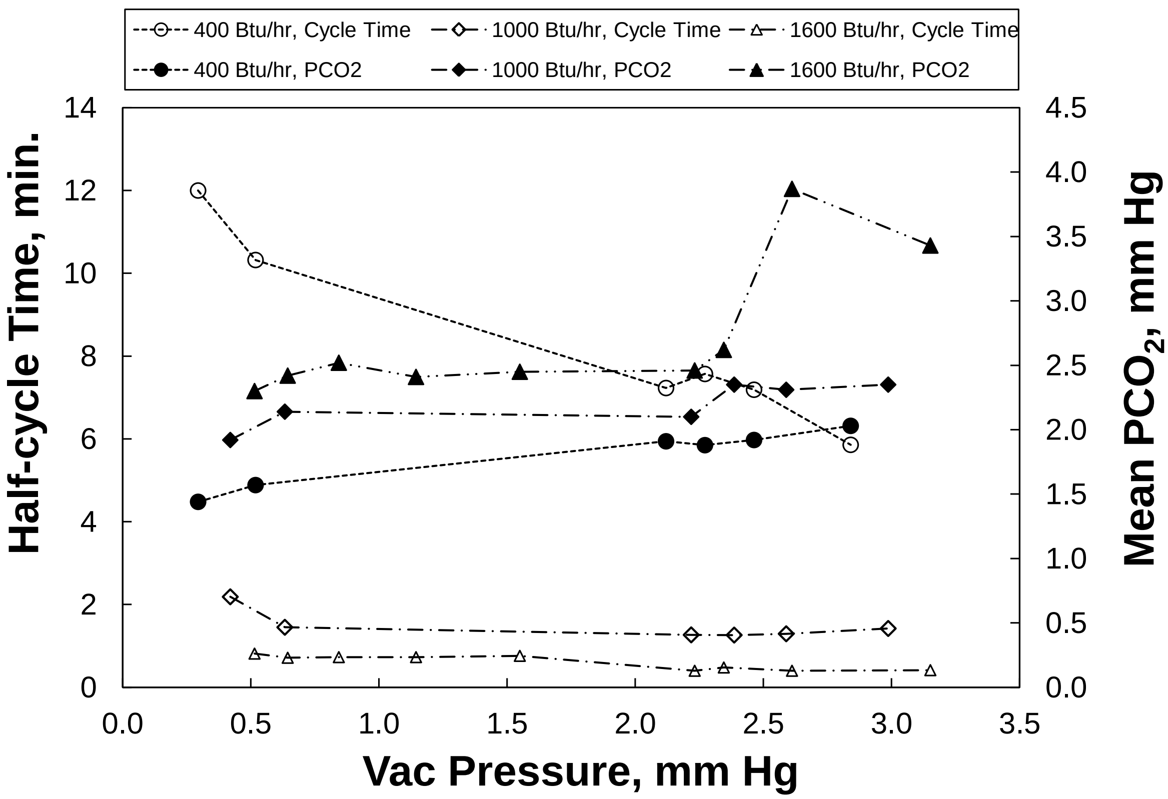

Figure 8: The influence of vacuum pressure on RCA performance. Open markers are associated with half-cycle time whereas closed markers indicate the mean partial pressure for the provided metabolic rate. Test conditions include various metabolic rates, 4.1 psia loop pressure, a 6.0 acfm flow rate, and a PGS volume simulator inlet cycle criteria of 3.3 mm Hg.

result, it is worth considering calculating metabolic rate during EVA using other data such as a change in partial pressure across the RCA or a temperature change across the liquid cooling ventilation garment. Discrepancy between calculated metabolic rates from half-cycle data and other techniques may provide a real-time diagnostic indicating whether the vacuum port has been plugged so that the crewmember can react accordingly. However, in spite of significantly compromising the vacuum quality during testing, the results in Fig. 7&8 demonstrate the RCA is still capable of revitalizing the atmosphere within the ventilation subsystem albeit with decreased half-cycle time thereby increasing expected ullage losses during EVA.

E. Deliberate Failure and Recovery Experiment

The RCA within the ventilation loop responsible for removing carbon dioxide and water vapor has been tested under nominal conditions, through off-nominal high metabolic rates, transient metabolic profiles, with increased humidity, and with degraded vacuum. In all scenarios, the RCA has demonstrated the capability to perform per requirements. However, the RCA itself has not been investigated for a direct test article failure. The objective of this analysis was to deliberately power off the RCA spool valve, monitor the increase in CO_2 and H_2O vapor, and then power the valve on to see how quickly the RCA can react to this type of a failure. During actual EVA, the crewmember would likely immediately enter the purge mode contingency operational scenario. Nevertheless, it was of interest to see how the RCA would respond to CO_2 and H_2O concentrations far beyond what would plausibly be expected to exist within the spacesuit should such an unexpected event arise. Such results are demonstrated in Fig. 9.

The results in Fig. 9 demonstrate the capacity of the RCA to overcome valve failure and to revitalize a ventilation stream starting at a point containing significant amounts of CO_2 and H_2O vapor. During the

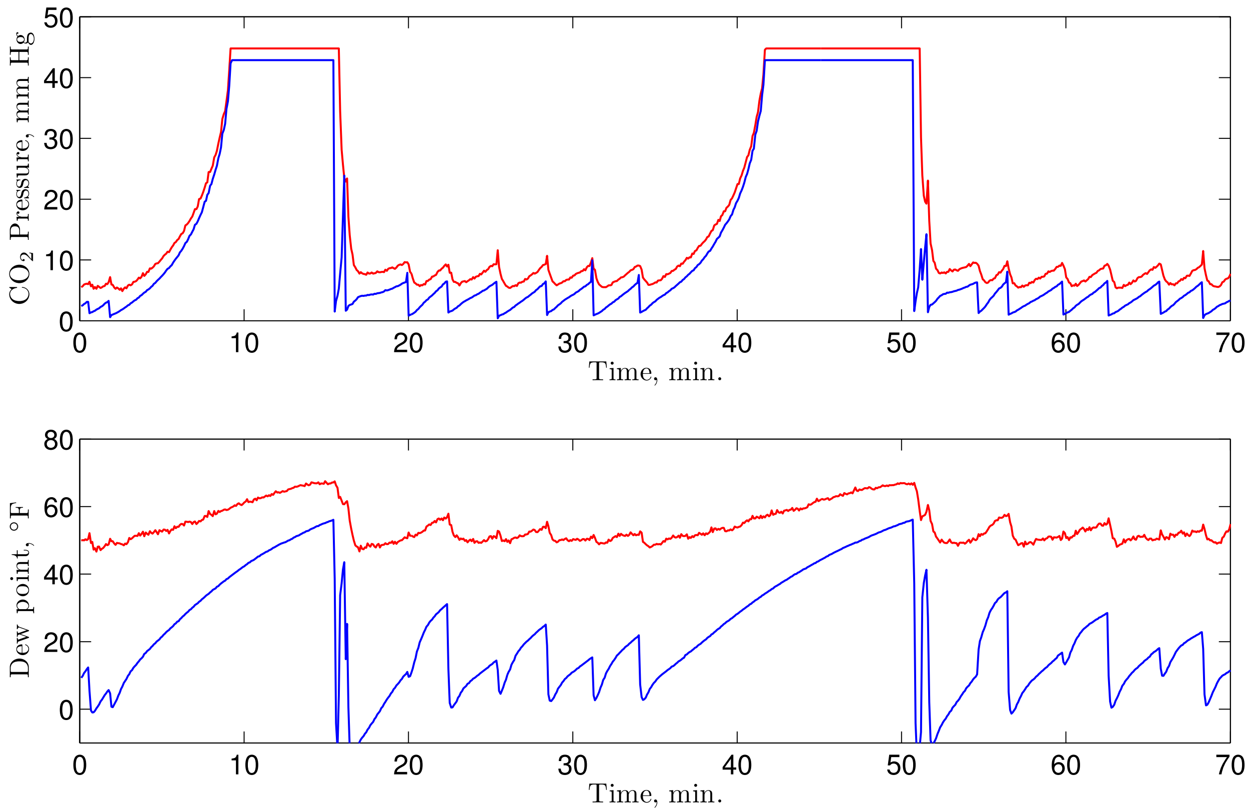

Figure 9: Deliberate failure and recovery experiment. Test conditions included a metabolic rate of 1000 Btu/hr, 4.1 psia loop pressure, and a 4.5 acfm flow rate. During the recover phases, the RCA valve was cycled when the PGS volume simulator inlet CO_2 partial pressure reached 6.0 mm Hg.

experiment, a 1000 Btu/hr profile was allowed to achieve cyclic steady-state. Once this occurred, the valve was powered off for approximately 15 minutes while CO_2 partial pressure increased to the point it went off-scale high according to the Li-Cor 840A gas analyzers (between 40–50 mm Hg). The experiment continued as the dew point within the test loop approached ambient temperature. After 15 minutes, the valve was powered on once again and the RCA was operated to cycle at an instantaneous threshold of 6.0 mm Hg which has been the traditional method of control.[7] A delay of 20 seconds was imposed on the controller before allowing it command the spool valve to cycle again, thereby preventing the RCA from immediately cycling back and forth without enabling time to scrub the ventilation stream (a term we refer to as 'short-cycling'). After enabling the valve to function once again, the saturated bed was immediately switched into vacuum regeneration model while the fresh bed began scrubbing the ventilation stream. Within the 20 second delay, bed breakthrough occured and concentration out of the RCA increased beyond 20 mm Hg. After 20 seconds, the valve cycled once again to the regenerated bed. Within this third cycle, the RCA was able to recover and control to the 6.0 mm Hg threshold. By the fourth cycle, the RCA was once again approaching cyclic steady-state. This experiment was repeated once again at around 35 minutes with similar results. Moreover, although not displayed within this report, the experiment was repeated with a threshold of 3.0 mm Hg with similar results. In addition, this experiment was also performed for a metabolic rate of 1600 Btu/hr with similar results. In aggregate, these experiments demonstrate the capability of the RCA to recover from either a temporary valve failure or a loss of power to the PLSS. Consequently, these results provide confidence that the advanced PLSS under development is robust and fault tolerant.

IV. Conclusions

For the first time in decades, the PLSS of the EMU is undergoing a major re-design. The advanced PLSS under development employs several new technologies to provide variable pressure regulation, regenerable air revitalization, and robust thermal control. These new technologies simplify the PLSS schematic, minimize consumables, reduce subsystem criticality, and decrease system mass and volume. Prior to 2011, most of these technologies were tested only at the component level. The PLSS 1.0 test marks the first time the advanced PLSS has been configured to assess the performance of the individual components in an integrated context. Packageability was sacrificed for increased instrumentation for performance characterization for these tests. The results thereof are described within this manuscript.

The primary objective to demonstrate performance across multiple pressures, metabolic rates, and loop flow rates was demonstrated first. These tests provided data to verify that the test stand was functioning correctly and that the advanced PLSS could meet performance requirements. In all cases, the integrated PLSS accomplished requirements; in part, due to the on-back regenerable RCA vacuum swing bed within the ventilation subsystem.

Simulated EVA variable metabolic rate tests were performed following single metabolic rate experiments. As an added challenge to the RCA, the cycle criterion was decreased to 3.0 mm Hg and the mean metabolic rate was increased from an expected nominal EVA rate to 1330 Btu/hr. This is a significant challenge to the advanced PLSS. In some cases, metabolic rates as high as 3070 Btu/hr were simulated. The RCA again demonstrated the capability to revitalize to achieve requirements.

An exploration of conceivable off-nominal and contingency conditions were explored after performance under a wide variety of metabolic challenges had been demonstrated. The RCA showed a capability to remove significant amounts of moisture from the atmosphere during high humidity cases. In the highest humidity test where water vapor was introduced at roughly two-fold the expected metabolic equivalent, the RCA removed significant moisture from the atmosphere although it is worth noting that test data suggests condensation may have occurred within the test loop. In spite of possible condensation, the RCA was capable of scrubbing the water vapor from the ventilation stream at humidities near 100%.

Loss of vacuum quality was also investigated presumably simulating a clogged or compromised vacuum line. In this analysis, minimum vacuum pressure was increased from 0.29 mm Hg to just around 3.0 mm Hg. To the best knowledge of the authors, this represents the highest degraded vacuum test for the SA9T material within the interleaved canister design. In the degraded vacuum test, the RCA again proved capable of providing life support functions even though deliberately compromised, thus indicating the RCA is a robust option to replace the LiOH/MetOx canisters and condensing heat exchanger in the current PLSS. Even though the RCA met requirements in these tests, the degraded vacuum data also helped demonstrate the importance of reaching sub-Torr pressures to remove significant amounts of sorbed CO_2.

Lastly, a failed valve or loss of PLSS power was simulated without the purge mode as a worst-case investigation to monitor how the RCA would respond after receiving power once again. In these test points, CO_2 partial pressure was increased well beyond 40 mm Hg before actuating the RCA spool valve. The RCA was able to respond and achieve a cyclic steady-state once again in around 3–4 cycles. These results indicate that RCA is capable recovering from a failed state even when CO_2 and moisture are in gross excess.

These results demonstrate a robust and flexible life support system from the standpoint of developmental efforts for the advanced PLSS. The integrated test represents a major milestone in the roadmap toward replacing the current state-of-the-art. Although integrated performance has been proven, the highly instrumented system was far larger than could be packaged upon an EMU. Consequently, efforts are underway to design and build a packaged integrated system for terrestrial vacuum chamber testing. The advanced PLSS team looks forward to reporting these efforts in the near future.

References

[1]Chullen, C. and Westheimer, D., "Extravehicular Activity Technology Development Status and Forecast," *41st International Conference on Environmental Systems*, Am. Inst. Astronaut. & Aeronaut., Portland, OR, 2011, Paper No. 2011–5179.

[2]Chullen, C., McMann, J., Dolan, K., Bitterly, R., and Lewis, C., "U.S. Spacesuit Knowledge Capture," *41st International Conference on Environmental Systems*, Am. Inst. Astronaut. & Aeronaut., Portland, OR, 2011, Paper No. 2011–5199.

[3]Westheimer, D. and Chullen, C., "Extravehicular Activity Technology Needs," *AIAA Space 2010 Conference & Exposition*, Am. Inst. Astronaut. & Aeronaut., Anaheim, CA, 2010, Paper No. 2010–8651.

[4]Goeppert, A., Czaun, M., May, R., Prakash, G., Olah, G., and Narayanan, S., "Carbon Dioxide Capture from the Air Using a Polyamine Based Regenerable Solid Adsorbent," *Journal of the American Chemical Society*, 2011.

[5]Birbara, P., Filburn, T., Michels, H., and Nalette, T., "Sorbent system and method for absorbing carbon dioxide (CO2) from the atmosphere of a closed habitable environment," April 2002, US Patent 6,364,938.

[6]Chang, A., Chuang, S., Gray, M., and Soong, Y., "In-situ infrared study of CO2 adsorption on SBA-15 grafted with γ-(aminopropyl) triethoxysilane," *Energy & Fuels*, Vol. 17, No. 2, 2003, pp. 468–473.

[7]Papale, W., Paul, H., and Thomas, G., "Development of Pressure Swing Adsorption Technology for Spacesuit Carbon Dioxide and Humidity Removal," *Proceedings of the International Conference on Environmental Systems*, SAE International, Norfolk, VA, 2006, Paper No. 2006-01-2203.

[8]McMillin, S., Broerman, C., Swickrath, M., and Anderson, M., "Testing and Results of Vacuum Swing Adsorption Units for Spacesuit Carbon Dioxide and Humidity Control," *41st International Conference on Environmental Systems*, Am. Inst. Astronaut. & Aeronaut., Portland, OR, 2011, Paper No. 2011–5244.

[9]Swickrath, M., Anderson, M., McMillin, S., and Broerman, C., "Simulation and Analysis of Vacuum Swing Adsorption Units for Spacesuit Carbon Dioxide and Humidity Control," *41st International Conference on Environmental Systems*, Am. Inst. Astronaut. & Aeronaut., Portland, OR, 2011, Paper No. 2011–5243.

[10]Bue, G., Makinen, J., Vogel, M., Honas, M., Dillon, P., Colunga, A., Truong, L., Poritz, D., and Tsioulos, G., "Hollow Fiber Flight Prototype Spacesuit Water Membrane Evaporator Design and Testing," *41st International Conference on Environmental Systems*, Am. Inst. Astronaut. & Aeronaut., Portland, OR, 2011, Paper No. 2011–5259.

[11]Bue, G., Trevino, L., Tsioulos, G., Settles, J., Colunga, A., Vogel, M., and Vonau, W., "Hollow Fiber Spacesuit Water Membrane Evaporator Development and Testing for Advanced Spacesuits," *40th International Conference on Environmental Systems*, Am. Inst. Astronaut. & Aeronaut., Barcelona, Spain, 2010, Paper No. 2010–6040.

[12]Vogel, M., Vonau, W., Trevino, L., and Bue, "Sheet Membrane Spacesuit Water Membrane Evaporator Design and Thermal Tests," *40th International Conference on Environmental Systems*, Am. Inst. Astronaut. & Aeronaut., Barcelona, Spain, 2010, Paper No. 2010–6039.

[13]NASA, "Constellation Program Human-Systems Integration Requirements," Tech. Rep. CxP 70024, NASA, 2009.

[14]James, J., Meyers, V., Sipes, W., Scully, R., and Matty, C., "Crew Health and Performance Improvements with Reduced Carbon Dioxide Levels and the Resource Impact to Accomplish Those Reductions," *41st International Conference on Environmental Systems*, Am. Inst. Astronaut. & Aeronaut., Portland, OR, 2011, Paper No. 2011–5047.

[15]Ball, T. and Straus, J., "Space Suit Helmet CFD Analysis Results utilizing a Sinusoidal Breathing Model," *41st International Conference on Environmental Systems*, Am. Inst. Astronaut. & Aeronaut., Portland, OR, 2011, Paper No. 2011–5054.

[16]Thomas, G., Schneider, S., Keilich, M., and Conger, B., "Crew Member/Extravehicular Mobility Unit Thermal Interactions Affecting Cooling Preferences and Metabolic Water Removal," *25th International Conference on Environmental Systems*, SAE International, San Diego, CA, 1995, Paper No. 951637.

[17]Adamson, A. and Gast, *Physical chemistry of surfaces*, Wiley, New York, 1997.

[18]LeVan, M., Carta, G., and Yon, M., "Chap. 16: Adsorption and Ion Exchange," *Perry's chemical engineers' handbook*, McGraw-Hill New York, 7th ed., 1997.